Electronic Supplementary Information

Optimizing Mannose "Click" Conjugation to Polymeric Nanoparticles for Targeted siRNA Delivery to Human and Murine Macrophages

Evan B. Glass[§•], Shirin Masjedi[§•], Stephanie O. Dudzinski[§•], Andrew J. Wilson[‖], Craig L. Duvall[§•], Fiona E. Yull[‡‖+], and Todd D. Giorgio*[§†+•]

[§]Department of Biomedical Engineering, Vanderbilt University, 5824 Stevenson Center, Nashville, TN 37232, USA.

[‡]Department of Pharmacology, Vanderbilt University, Nashville, TN 37232, USA.

Department of Obstetrics & Gynecology, Vanderbilt University Medical Center, Nashville, TN 37232, USA.

[†]Department of Chemical and Biomolecular Engineering, Vanderbilt University, Nashville, TN 37232, USA.

[+]These authors provided equal contributions.

Supplementary Materials & Methods

Mannose-Alkyne Synthesis

Briefly, D-mannose (Mn, 2g) was dissolved in dimethyl sulfoxide (DMSO) (20 mL, 10% w/v) in a 25 mL round bottom flask with a stir bar. The flask was sealed with a rubber top, placed on a stir plate, and purged with nitrogen (N_2 (g)) for 30 minutes while stirring. While purging, triethylamine (TEA, 1.082 mL) was added to activate the sugar into a nucleophile before propargyl bromide (0.547 mL) was added. Both TEA and propargyl bromide were added using a needle and syringe to prevent oxygen from leaking into the reaction vessel. The final molar ratio of mannose:TEA:propargyl bromide was 60:72:67 moles. After removing the nitrogen purge, the solution was heated to 40°C in an oil bath and stirred for 24 hours. The final solution was added to equal volume diethyl ether for extraction of excess reagents. The leftover ether was disposed and the resulting DMSO solution was collected. This extraction was repeated 5x. The final DMSO was mixed with equal volume nuclease-free water (Thermo Fisher Scientific, Waltham, MA) and extracted into equal volume dichloromethane to remove other byproducts as well as DMSO. Once again, this extraction was performed 5x. The final mannose-alkyne solution in nuclease-free water was collected, frozen at -80°C, and lyophilized. Synthesis of mannose-alkyne has been previously characterized and we confirm successful alkyne functionalization with 1H-NMR (**Supplemental Figure S2**).[1] Although the reaction scheme depicts alkyne conjugation to a particular hydroxyl group, this reaction is not specific for only that hydroxyl. Near-random conjugation among hydroxyls is not anticipated to affect binding to CD206 since this receptor primarily binds mannose-like structures on bacterial cell walls.[1,2]

Fabrication of Macro-CTA for RAFT

All polymers were fabricated using 4-cyano-4-(ethylsulfanylthiocarbonyl)-sulfanylpentanoic acid (ECT) as a chain transfer agent (CTA). ECT was synthesized as previously described.[3,4] A 5 kDa hydroxyl PEG azide (500 mg, AzPEG, Polysciences, Inc., Warrington, PA) was reacted with ECT to form a macro-CTA suitable for RAFT polymerization. AzPEG was dissolved in dichloromethane (DCM) (5 mL) and mixed with 4-dimethylaminopyridine (DMAP) (30.2 mg, molar ratio 2.5:1 DMAP:AzPEG). Separately, ECT (130 mg) was dissolved in DCM (5 mL) at a 5:1 molar excess to AzPEG (accounting for total volume when combined). N,N'-dicyclohexylcarbodiimide (DCC, 102 mg) was added to the ECT solution at a 5:1 molar excess to the AzPEG. The ECT/DCC solution was added to a 25 mL round bottom flask with a N_2 balloon purge and stirred for 5 minutes to allow the DCC to activate the carboxylic acid group of the ECT. The AzPEG/DMAP solution was then added and the total solution (10 mL, 5% w/v AzPEG) was covered with aluminum foil and stirred for 48 hours at room temperature. After reacting, the solution was purified by dialyzing against methanol for 24 hours followed by dialyzing against deionized (DI) water for 24 hours using a 3.5 kDa-MWCO membrane.[5,6] The final solution was frozen at -80°C and lyophilized. Conjugation of ECT to the AzPEG was confirmed with 1H-NMR as previously described (**Supplemental Figure S3**).[5]

RAFT Polymerization of Diblock Copolymers

The AzPEG and PEG macro-CTAs were then RAFT polymerized with DMAEMA and BMA at a 50:50 molar ratio as previously described.[1,5,7] The macro-CTA (150 mg) was dissolved in dioxane (8.39 mL, 14% w/v) with recrystallized 2,2′-azobis(2-methylpropionitrile) (AIBN) as the initiator (0.47 mg, 10:1 CTA:initiator molar ratio). Based on previous experience with the diblock copolymer, overall best performance was generally obtained from a polymer with approximately 120-140 monomers.[5] Previous syntheses with similar systems produced a conversion rate of 60-65% so we designed the reaction at a degree of polymerization of 240. DMAEMA (576 µL) and BMA (543 µL) were added at 50:50 mol% and the entire solution was placed in a 50 mL round bottom flask and sealed with a rubber stopper. The solution was purged with N_2 for 30 minutes and then placed in an oil bath at 70°C for 24 hours. After completion of the reaction, the AzPEG(DMAEMA-co-BMA) (AzPEGDB) and PEGDB solutions were dialyzed for 24 hours in methanol and 24 hours in DI water using a 3.5 kDa-

MWCO membrane. The solutions were then frozen and lyophilized for long-term storage. Fabrication of the PEG-ECT macro-CTA and subsequent RAFT polymerization of PEGDB has been previously well-characterized.[5,6,8–10]

Alkyne-Azide "Click" Functionalization

AzPEGDB (250 mg) was dissolved in 10% (v/v) 200-proof ethanol and 90% nuclease-free water (25 mL total, 10 mg/mL) in a 100 mL round bottom flask. Then, mannose-alkyne (5.93 mg, 1:3 azide:alkyne molar ratio) and sodium ascorbate (24.8 mg, 5 mM) were added to the reaction vessel. The copper catalyst (copper sulfate ($CuSO_4$)) was added at concentrations of 0.1, 0.25, 0.5, 0.75, or 1 mM (0.62 mg, 1.56 mg, 3.12 mg, 4.68 mg, 6.24 mg, respectively) to examine conjugation efficiency at different catalyst concentrations. The reaction vessel was sealed with a rubber stopper and placed on a stir plate for 48 hours at room temperature. Post-reaction, a Chelex resin (1.25 g, 5 g/100 mL, Bio-Rad, Hercules, CA) was added and stirred for 2 hours to remove residual Cu^{2+} ions. The solution was filtered through a 0.45 µm filter to remove the Chelex resin and dialyzed against DI water for 24 hours using a 3.5 kDa-MWCO membrane. The purified solution was frozen at -80°C and lyophilized.

Figure S1: Polyplex Toxicity in ThP-1 Human Macrophages

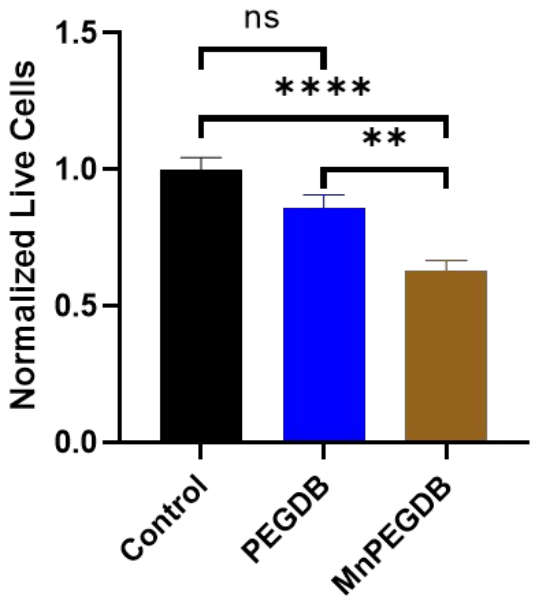

Supplemental Figure S1: Viability studies with ThP-1 human macrophages treated with PEGDB and MnPEGDB (prepared with 1 mM copper catalyst) revealed a significant toxic effect in the MnPEGDB group, which we hypothesized to be caused by residual copper from CuAAC.

Figure S2: Mannose-Alkyne Fabrication

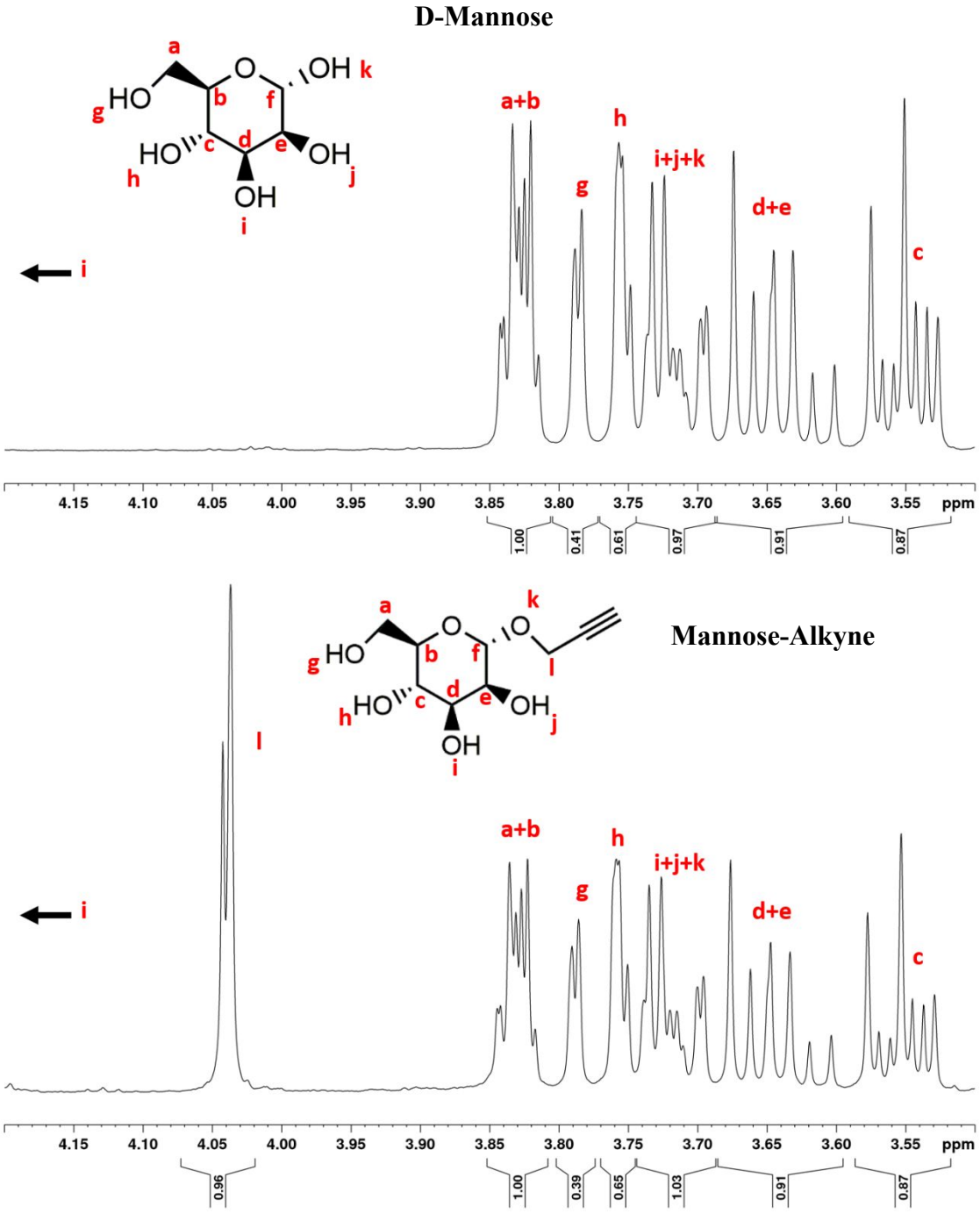

Supplemental Figure S2: ^{1}H-NMR of mannose functionalization with propargyl bromide to form mannose-alkyne, performed in D_2O. Successful conjugation is confirmed by the appearance of the alkyne peak at δ 4.04s. Integration of peaks reveals a 1:1 conjugation efficiency. These results match previous data from our lab. Note that alkyne conjugation to mannose is not expected to be specific for a particular hydroxyl group.

Figure S3: Azide-PEGDB Fabrication

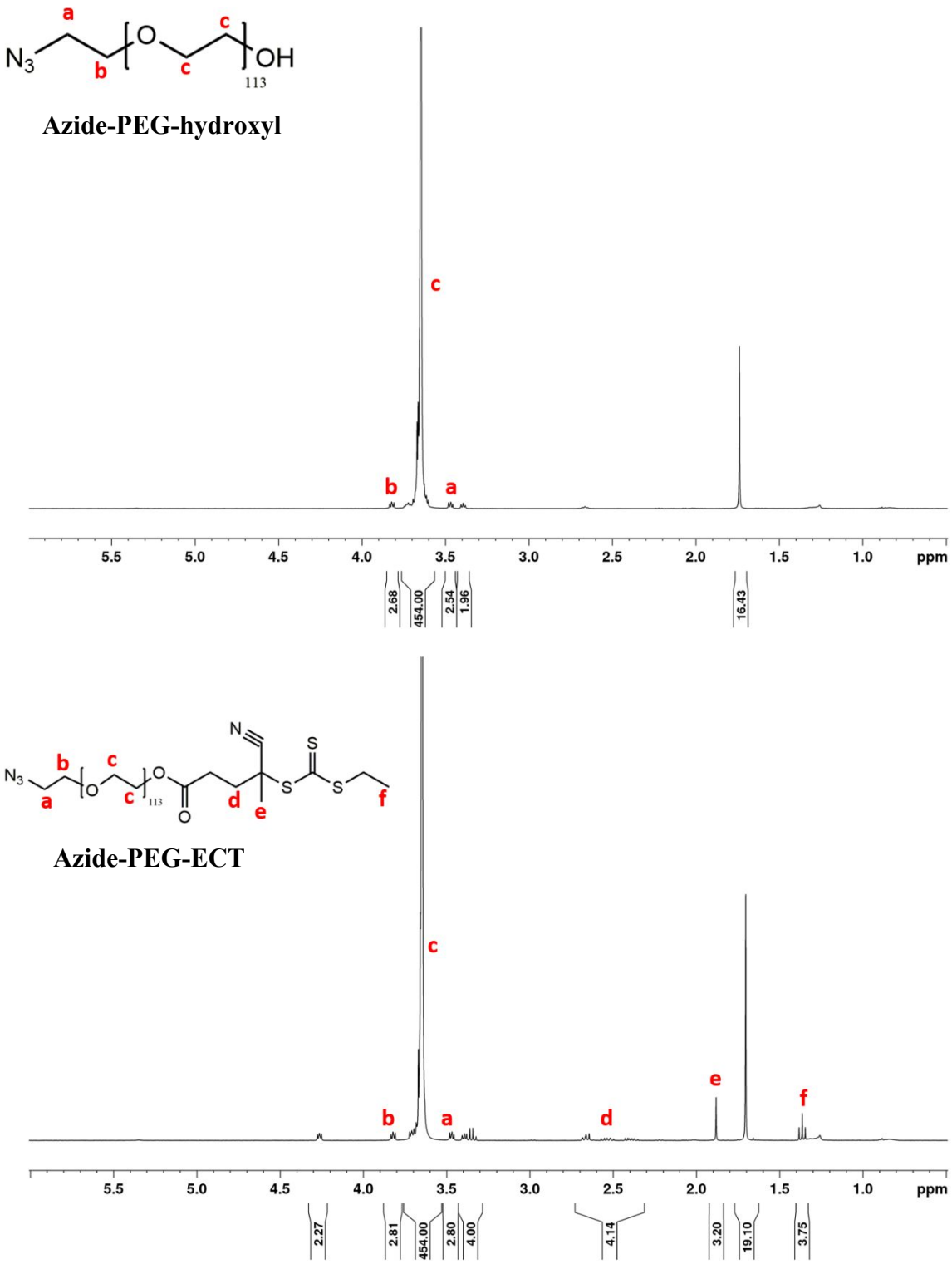

Supplementary Figure S3: [1]H-NMR of Azide-PEG-DB reaction steps in CDCl3 – continued on next page.

Figure S3: Azide-PEGDB Fabrication (Continued)

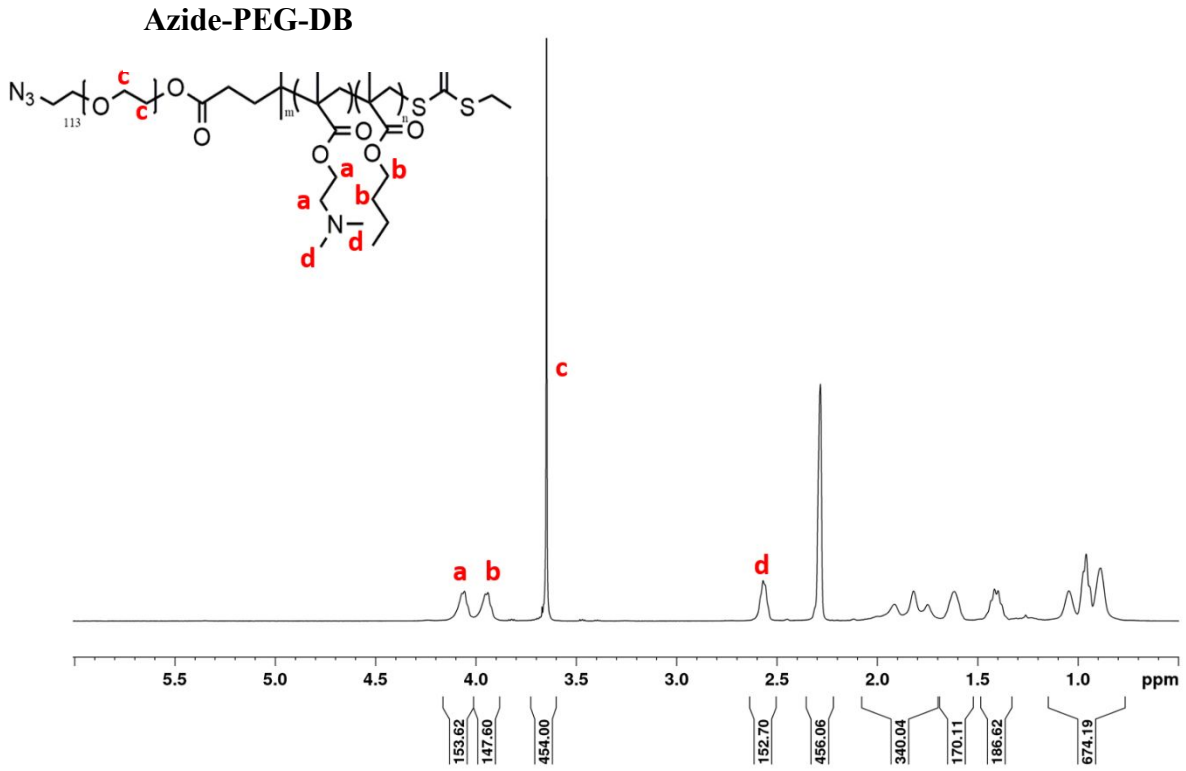

Supplemental Figure S3: ^{1}H-NMR of each reaction step in CDCl3. Azide-PEG-hydroxyl is reacted with the ECT macro-CTA to create Azide-PEG-ECT. Azide-PEG-ECT maintains the characteristic PEG peak at δ 3.65s (-OC**H**$_2$C**H**$_2$-) and adds the ECT peak δ 1.88s (CCNC**H**$_3$). RAFT polymerization produces AzPEGDB, which is confirmed by the DMAEMA (δ 4.05s, -OC**H**$_2$CH$_2$-) and BMA (δ 3.95s, -OC**H**$_2$CH$_2$-) peaks. Polymer repeating units for AzPEGDB were calculated by calibrating the PEG peak to the number of hydrogens in the polymer and comparing to the DMAEMA and BMA peak integrals. Overall spectra of AzPEGECT and AzPEGDB match previously reported data using a similar polymer system.

Figure S4: MnPEGDB Polymers Fabricated with Various Copper Catalyst Concentrations

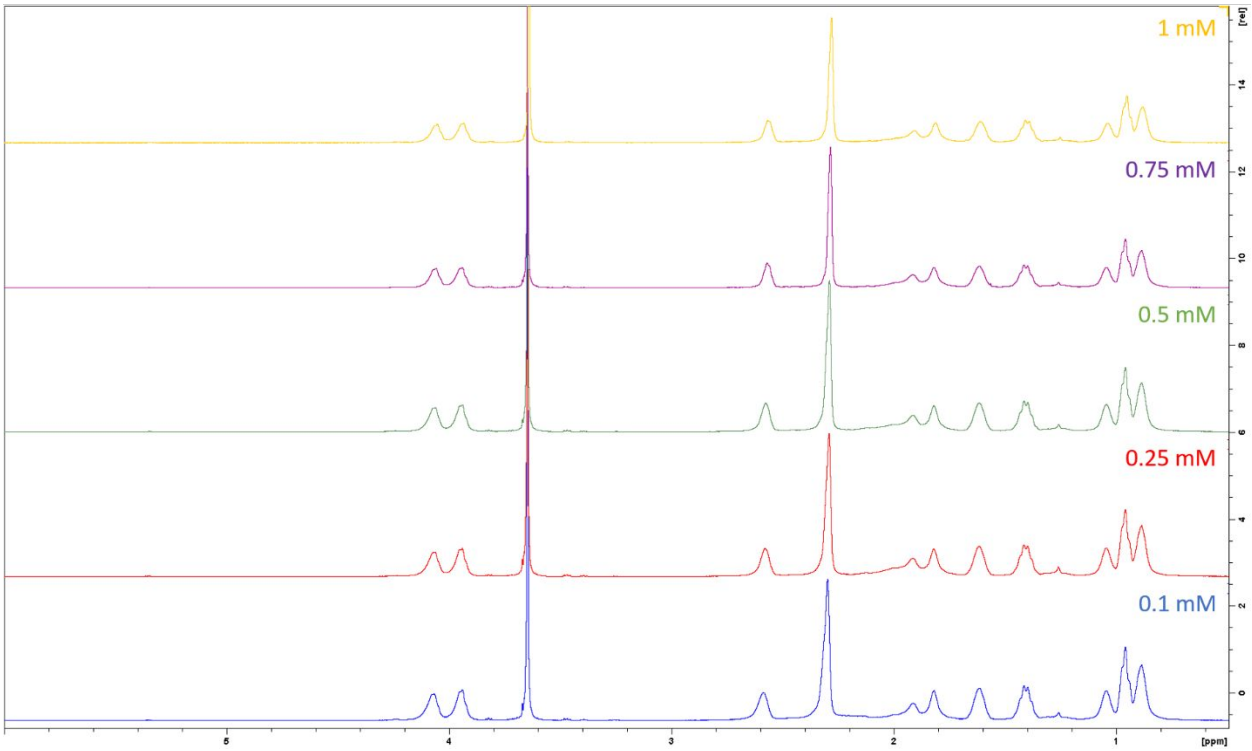

Supplemental Figure S4: ^{1}H-NMR of MnPEGDB polymers in CDCl3. All spectra matched between groups, indicating no changes in overall polymer structure despite changing the copper catalyst concentration in the CuAAC reaction. Note that mannose is not detectable with NMR since the peaks (shown in Figure S2) overlap with the PEG peak, which has 113 repeating units per polymer compared to one for mannose.

Table S1: RT-PCR Primer Sequences

Gene name	Forward sequence	Reverse sequence
CD86	TCTCCACGGAAACAGCATCT	CTTACGGAAGCACCCATGAT
TNF-α	CCCTCACACTCAGATCATCTTCT	GCTACGACGTGGGCTACAG
iNOS	TTCACCCAGTTGTGCATCGACCTA	TCCATGGTCACCTCCAACACAAGA
CD206	GCTCTTACTGACTGGCATGAG	CGCAGCTCTAGGAGCATGTG
IκBα	GAGCTCCGAGACTTTCGAGG	AGACACGTGTGGCCATTGTA
F4/80	CTTTGGCTATGGGCTTCCAGTC	GCAAGGAGGACAGAGTTTATCGTG
GAPDH	CCCTTAAGAGGGATGCTGCC	TACGGCCAAATCCGTTCACA
Actin-β	TATAAAACCCGGCGGCGCA	TCATCCATGGCGAACTGGTG

Table S2: Characterization of Polyplex Diameter, Homogeneity, and Surface Charge

Polymer	Avg Diameter (d.nm)	PDI	Avg Zeta Potential (mV)
PEGDB	140 ± 16	0.287	-0.142 ± 0.471
0.1 mM MnPEGDB	146 ± 18	0.273	-0.111 ± 0.347
0.25 mM MnPEGDB	148 ± 17	0.254	-0.332 ± 0.398
0.5 mM MnPEGDB	145 ± 12	0.259	-0.286 ± 0.438
0.75 mM MnPEGDB	151 ± 16	0.262	0.249 ± 0.054
1 mM MnPEGDB	151 ± 14	0.300	-0.417 ± 0.430

Figure S5: Flow Cytometry Gating Strategy and Polarized Macrophage Characterization

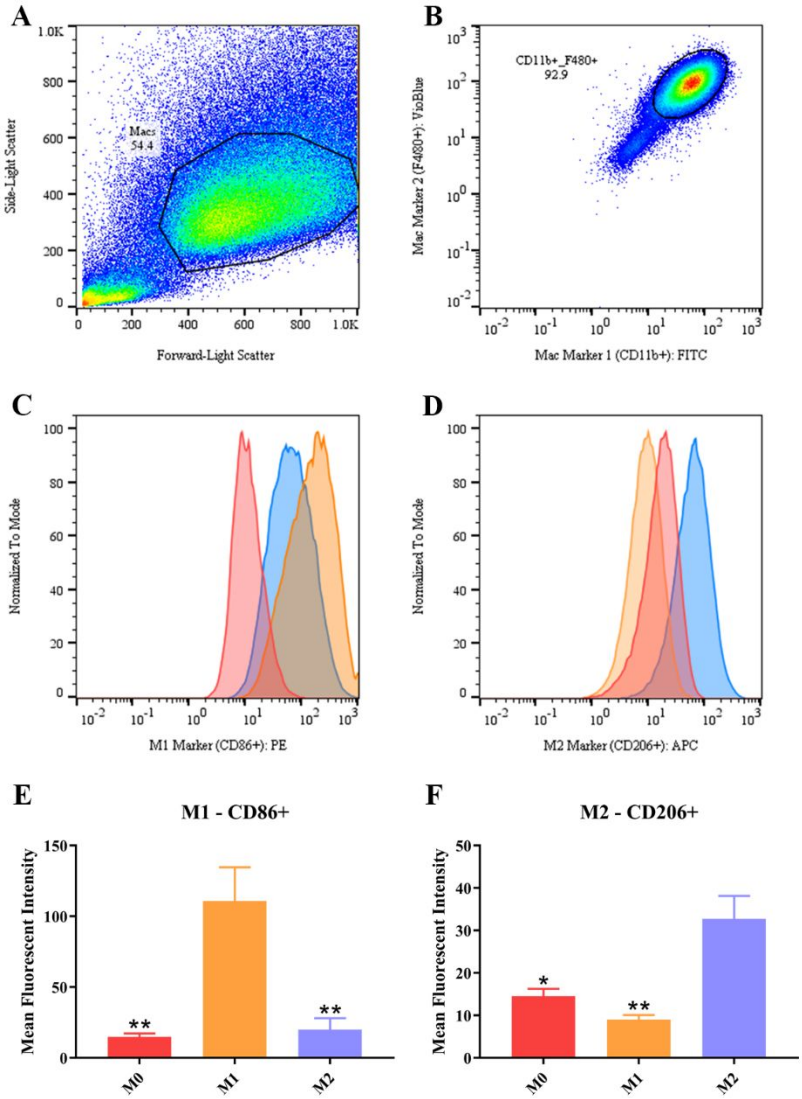

Supplementary Figure S5: (**A**) Gating of overall cell population in flow cytometry based on side-light scatter intensity vs forward-light scatter intensity. (**B**) Gating of macrophages determined by a double-positive population expressing F4/80 and CD11b. (**C,D**) Histogram plots depicting expressions of M1 (CD86) and M2 (CD206) markers on the different macrophage phenotypes. (**E**) CD86 was significantly increased in the M1-polarized macrophages compared to both M0 and M2 (**F**) CD206 was significantly overexpressed in M2 BMDMs.

Figure S6: Polyplex and Copper Toxicity in Human and Murine TNBC Cells and Human Mammary Epithelial Cells

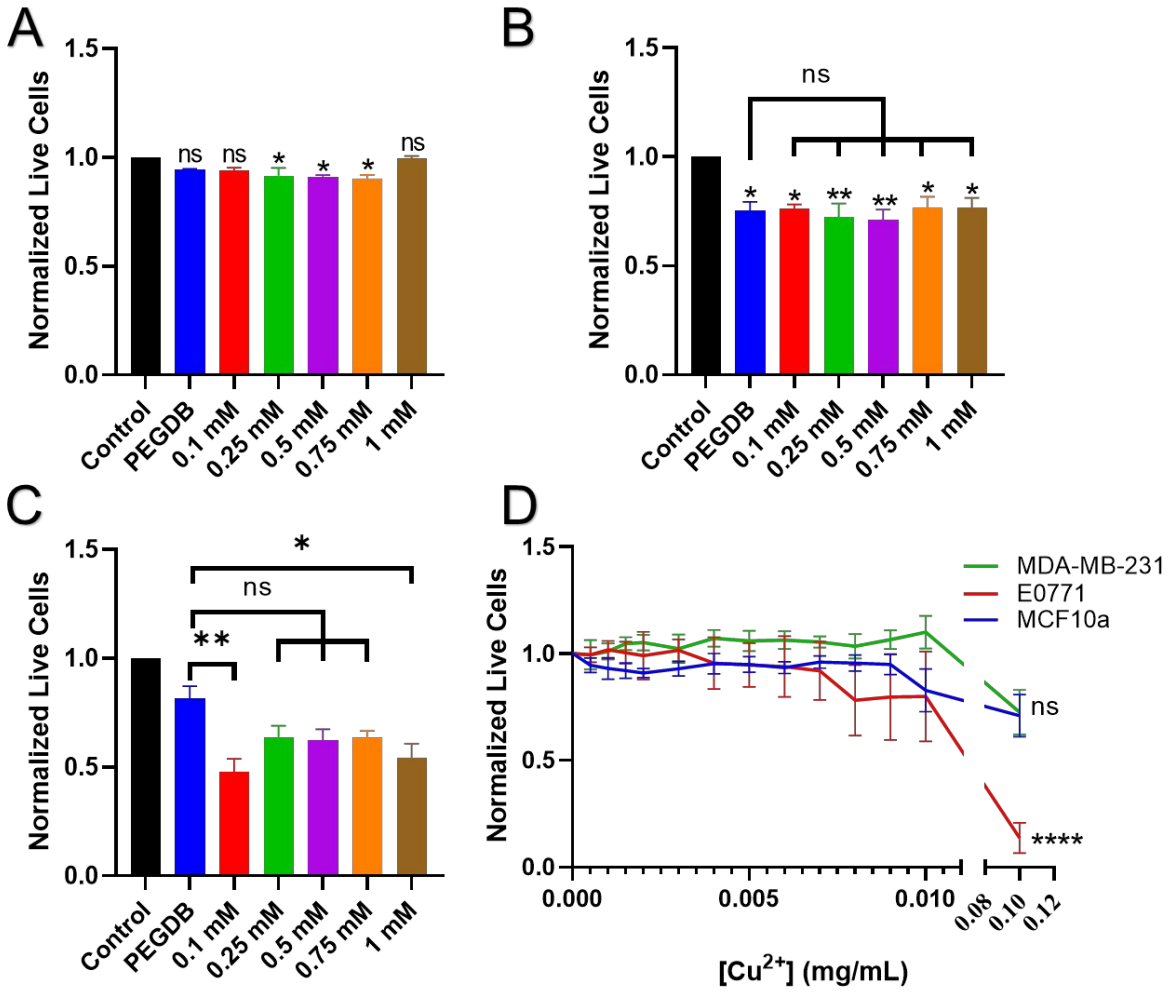

Supplementary Figure S6: (**A**) MDA-MB-231 human TNBC cells significantly decreased in viability in the 0.25-0.75 mM-prepared MnPEGDB polyplexes compared to untreated control, but still had viability greater than 90%. (**B**) E0771 murine TNBC cells had significantly less viability in all treatments compared to untreated control, but none of the MnPEGDB groups were significantly different from the PEGDB control polymer. (**C**) MCF10a human epithelial cells treated with 0.1 and 1 mM MnPEGDB were significantly less viable than the PEGDB control polymer, but the 0.25-0.75 mM groups were not significantly different. (**D**) All three cell types exhibited a trend of decreasing viability with increasing copper salt concentration, but only the E0771 murine TNBC cells had a significant change in viability at the highest concentration.

Figure S7: CD206-Specific Uptake of Polyplexes Confirmed via Co-Incubation with Free Mannose

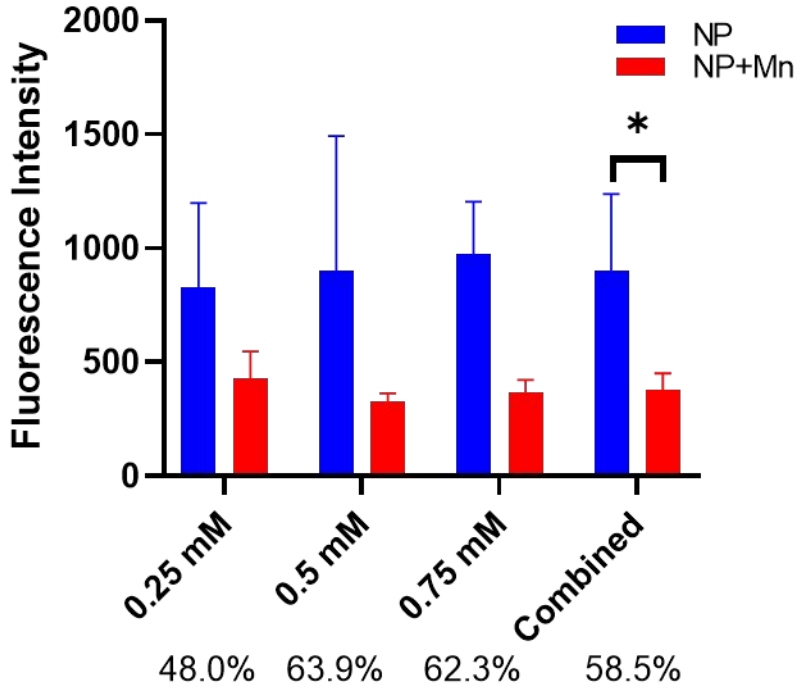

Supplementary Figure S7: M2-polarized BMDMs were treated with either mannose-decorated nanoparticles (NP) or NPs plus free mannose (NP+Mn). Fluorescence intensity revealed that all three of the optimal polymer formulations resulted in decreased uptake after adding free mannose (n=2). An average of the three optimal groups (combined, n=6) revealed a significant decrease in uptake with about 59% decrease due to mannose blocking the CD206 receptor.

Figure S8: Polyplex Uptake in TNBC Cells and Mammary Epithelial Cells

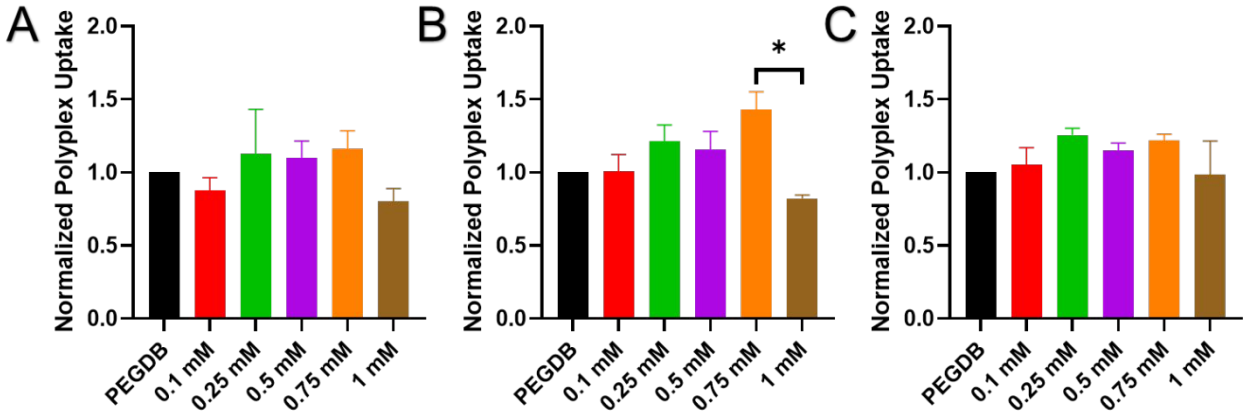

Supplementary Figure S8: (**A**) MDA-MB-231 cells had no significant changes in uptake regardless of mannosylation or copper content, indicating non-specific uptake of particles. (**B**) E0771 cells only exhibited a significant change in uptake between the 0.75 and 1 mM groups, but no other groups were different from each other. (**C**) MCF10a cells also displayed non-specific uptake, with no polymer groups differing from each other.

Supplemental Information References

(1) Yu, S. S.; Lau, C. M.; Barham, W. J.; Onishko, H. M.; Nelson, C. E.; Li, H.; Smith, C. A.; Yull, F. E.; Duvall, C. L.; Giorgio, T. D. Macrophage-Specific RNA Interference Targeting via "Click", Mannosylated Polymeric Micelles. *Mol. Pharm.* **2013**, *10* (3), 975–987. https://doi.org/10.1021/mp300434e.

(2) Azad, A. K.; Rajaram, M. V. S.; Schlesinger, L. S. Exploitation of the Macrophage Mannose Receptor (CD206) in Infectious Disease Diagnostics and Therapeutics. *J Cytol Mol Biol* **2014**, *1* (1), 1–10. https://doi.org/10.13188/2325-4653.1000003.

(3) Nelson, C. E.; Kim, A. J.; Adolph, E. J.; Gupta, M. K.; Yu, F.; Hocking, K. M.; Davidson, J. M.; Guelcher, S. A.; Duvall, C. L. Tunable Delivery of SiRNA from a Biodegradable Scaffold to Promote Angiogenesis In Vivo. *Adv. Mater.* **2014**, *26* (4), 607–506. https://doi.org/10.1002/adma.201303520.

(4) Convertine, A. J.; Benoit, D. S. W.; Duvall, C. L.; Hoffman, A. S.; Stayton, P. S. Development of a Novel Endosomolytic Diblock Copolymer for SiRNA Delivery. *J. Control. Release* **2009**, *133* (3), 221–229. https://doi.org/10.1016/j.jconrel.2008.10.004.

(5) Nelson, C. E.; Kintzing, J. R.; Hanna, A.; Shannon, J. M.; Gupta, M. K.; Duvall, C. L. Balancing Cationic and Hydrophobic Content of PEGylated SiRNA Polyplexes Enhances Endosome Escape, Stability, Blood Circulation Time, and Bioactivity in Vivo. *ACS Nano* **2013**, *7* (10), 8870–8880. https://doi.org/10.1021/nn403325f.

(6) Jackson, M. A.; Werfel, T. A.; Curvino, E. J.; Yu, F.; Kavanaugh, T. E.; Sarett, S. M.; Dockery, M. D.; Kilchrist, K. V; Jackson, A. N.; Giorgio, T. D.; et al. Zwitterionic Nanocarrier Surface Chemistry Improves SiRNA Tumor Delivery and Silencing Activity Relative to Polyethylene Glycol . *ACS Nano* **2017**, *11* (6), 5680–5696.

(7) Ortega, R. A.; Barham, W.; Sharman, K.; Tikhomirov, O.; Giorgio, T. D.; Yull, F. E. Manipulating the NF-KB Pathway in Macrophages Using Mannosylated, SiRNA-Delivering Nanoparticles Can Induce Immunostimulatory and Tumor Cytotoxic Functions. *Int. J. Nanomedicine* **2016**, *11*, 2163–2177. https://doi.org/10.2147/IJN.S93483.

(8) Miteva, M.; Kirkbride, K. C.; Kilchrist, K. V.; Werfel, T. A.; Li, H.; Nelson, C. E.; Gupta, M. K.; Giorgio, T. D.; Duvall, C. L. Tuning PEGylation of Mixed Micelles to Overcome Intracellular and Systemic SiRNA Delivery Barriers. *Biomaterials* **2015**, *38*, 97–107. https://doi.org/10.1016/j.biomaterials.2014.10.036.

(9) Werfel, T. A.; Jackson, M. A.; Kavanaugh, T. E.; Kirkbride, K. C.; Miteva, M.; Giorgio, T. D.; Duvall, C. Combinatorial Optimization of PEG Architecture and Hydrophobic Content Improves Ternary SiRNA Polyplex Stability, Pharmacokinetics, and Potency in Vivo. *J. Control. Release* **2017**, *255* (March), 12–26. https://doi.org/10.1016/j.jconrel.2017.03.389.

(10) Werfel, T. A.; Swain, C.; Nelson, C. E.; Kilchrist, K. V.; Evans, B. C.; Miteva, M.; Duvall, C. L. Hydrolytic Charge-Reversal of PEGylated Polyplexes Enhances Intracellular Un-Packaging and Activity of SiRNA. *J. Biomed. Mater. Res. - Part A* **2016**, *104* (4), 917–927. https://doi.org/10.1002/jbm.a.35629.